Signal Changes in the Brain on Susceptibility-Weighted Imaging Under Reduced Cerebral Blood Flow: A Preliminary Study

AUTHOR(S):

Fushimi, Yasutaka; Miki, Yukio; Mori, Nobuyuki; Okada, Tsutomu; Urayama, Shin-ichi; Fukuyama, Hidenao; Togashi, Kaori

CITATION:

Fushimi, Yasutaka ...[et al]. Signal Changes in the Brain on Susceptibility-Weighted Imaging Under Reduced Cerebral Blood Flow: A Preliminary Study. Journal of Neuroimaging 2010, 20(3): 255-259

ISSUE DATE:

2010-07

URL:

http://hdl.handle.net/2433/261985

Title Page

Signal Changes in The Brain on Susceptibility-weighted Imaging under Reduced Cerebral Blood Flow – A Preliminary Study –

Yasutaka Fushimi, M.D., Ph.D.[1), 2)] Yukio Miki, M.D., Ph.D.[1)], Nobuyuki Mori, M.D.[1)], Tsutomu Okada, M.D., Ph.D.[1) 3)], Shin-ichi Urayama, Ph.D.[4)], Hidenao Fukuyama, M.D., Ph.D.[4)], Kaori Togashi, M.D., Ph.D.[1)]

[1)] Department of Diagnostic Imaging and Nuclear Medicine, Kyoto University Graduate School of Medicine, Kyoto, Japan

[2)] Department of Radiology, Hikone Municipal Hospital, Hikone, Japan

[3)] Department of Radiology, Tenri Hospital, Tenri, Japan

[4)] Human Brain Research Center, Kyoto University Graduate School of Medicine, Kyoto, Japan

Running Title

SWI sensitively reflects hyperventilation-induced decreases in CBF.

Corresponding Author: Yukio Miki, M.D., Ph.D.

E-mail address: mikiy@kuhp.kyoto-u.ac.jp

54 Shogoin-Kawaharacho, Sakyo-ku, Kyoto, 606-8507, Japan

phone: 81-75-751-3710, fax: 81-75-771-9709

This study was supported in part by a Health and Labour Sciences Research Grant of Japan

Note: Yasutaka Fushimi and Yukio Miki equally contributed to the study.

Abstract

Objectives: To reveal the characteristics of susceptibility-weighted imaging (SWI) under low cerebral blood flow (CBF) induced by hyperventilation (HV).

Materials and Methods: This study was approved by the institutional review board. Informed consent was obtained. Six healthy volunteers (5 men, 1 woman; mean age, 29 years; range, 24-33 years) underwent SWI and arterial spin labeling perfusion imaging under normal ventilation (NV) and hyperventilation at 3.0 T. Regions of interest were placed on gray matter (GM) and white matter (WM) of the frontal lobe (FL) and occipital lobe (OL). Intensities of ROIs were compared between NV and HV. Contrast of veins compared with adjacent cerebral parenchyma (CV) was also compared between NV and HV.

Results: CBF during HV (CBF_{HV}) was decreased compared with CBF during NV (CBF_{NV}) (29.1 ±4.6%). FL-GM_{HV} and OL-GM_{HV} showed significant signal decreases compared with FL-GM_{NV} and OL-GM_{NV}, respectively (p=0.018, 0.017). CV_{HV} was significantly increased compared with CV_{NV} (164.1 ±29.9%) (p=0.00019).

Conclusions: SWI sensitively reflects HV-induced decreases in CBF. The present results might assist in the interpretation of SWI in clinical practice, since CBF decreases might also influence signal changes on SWI.

Text

Introduction

Susceptibility-weighted imaging (SWI) is a novel imaging method that maximizes the sensitivity to susceptibility effects of each voxel by using filtered phase images and magnitude images.[1, 2] Using high-resolution and fully flow-compensated images, SWI reveals vessels contiguity. SWI has been introduced to clinical use for examination of venous vasculatures,[1] vascular malformations [3] and tumor vascularities.[4] Since the technique is based on blood oxygen level-dependent (BOLD) contrast, SWI is also used for stroke [5] and hemorrhagic lesions.[6]

Increased oxygen extraction is needed to maintain oxygen metabolism under conditions of reduced cerebral blood flow (CBF), which decreases BOLD signals due to increased levels of deoxyhemoglobin in the venous blood.[7] BOLD signals are dependent on venous blood oxygenation, so many reports have featured BOLD signal changes associated with CBF, including under conditions of hypercapnia,[8-11] and hypocapnia.[12-15] Arterial partial pressure of CO_2 ($PaCO_2$) is an important regulator of cerebral circulation.[16] Hypercapnia is known to increase CBF by inducing vasodilatation.[9] Hypercapnia induces increases in BOLD signals, since increased CBF raises blood venous oxygenation.[8] Conversely, hypocapnia caused by hyperventilation

induces respiratory alkalosis, which increases perivascular pH. Increased perivascular pH causes vasoconstriction of cerebral vessels and decreased CBF.[15] On BOLD imaging hypocapnia decreases BOLD signals, which results in boosting BOLD contrast in event-related stimulation paradigms due to lower venous oxygenation.[12-14] Caffeine also decreases CBF by vasoconstriction of cerebral vessels,[17] subsequently boosts BOLD contrast due to BOLD signal decrease.[18, 19]

Rauscher et al [10] reported that SWI under hypercapnia caused by carbogen shows loss of contrast between veins and surrounding tissues due to higher blood oxygenation. They also showed significant increases in gray matter signals. Haacke, et al [20] reported that SWI using caffeine enhanced the resting state BOLD effect and the ability of SWI to image small vessels in the brain under decreased CBF. However, no reports have described SWI of the brain under hyperventilation (HV) induced hypocapnia. Evaluation of the signal characteristics of SWI under decreased CBF is important, particularly when clinical applications are planned for cerebral ischemic diseases. In most studies focusing on hyperventilation, proportions of CBF changes are not monitored, so the degree of CBF changes should be also clarified.

The aim of this study was to reveal the characteristics of SWI under HV induced low CBF.

Materials and Methods

Subjects comprised 6 healthy volunteers (5 men, 1 woman; mean age, 29 years; range, 24-33 years). All subjects were examined by the same neurologist and displayed no neurological abnormalities. Institutional review board approval was obtained for all study protocols, and all subjects provided written informed consent.

Ventilation Protocol

All subjects first underwent both SWI and arterial spin labeling (ASL) perfusion imaging under normal ventilation (NV), followed by SWI and ASL perfusion imaging under HV. Subjects were trained not to move their head during ventilations. Respiratory rate was maintained at around 10-15 breaths/min for NV and 20-30 breaths/min for HV by monitoring.

Data Acquisition

All subjects underwent SWI and ASL perfusion imaging in a whole-body 3T-MR scanner (Magnetom Trio; Siemens, Erlangen, Germany) using an integrated parallel acquisition technique and a receiver-only 8-channel phased-array head coil. The

generalized autocalibrating partially parallel acquisitions (GRAPPA) algorithm was applied for all sequences.

Imaging protocols

SWI used the following settings: repetition time (TR), 27 ms; echo time (TE), 20 ms; flip angle, 15°; field of view (FOV), 230 mm × 186 mm; matrix, 512 × 416; slice thickness, 0.9 mm; imaging slices, 22; and scan time, 122 s. To alleviate stress during hyperventilation, imaging slices were minimized and a relatively shorter scan time was achieved. Imaging center was set to the slice including the basal ganglia and frontal and occipital lobes.

ASL perfusion imaging (modified flow-sensitive alternating inversion recovery technique, pulsed ASL) used the following settings: TR, 2930 ms; TE, 27 ms; FOV, 200 mm × 200 mm; matrix, 64 × 64; slice thickness, 8 mm; slice selective inversion slab, 10 cm; duration of tagging bolus (TI_1), 700 ms; post-labeling delay, 800 ms; image acquisition carried out at TI_2 of 1500 ms; and 80 repetitions. The saturation pulse was applied to a 10-cm slab adjacent and inferior to the selective inversion slab in both label and control acquisitions. M0 images were also obtained for quantification.[21]

Imaging Processing

For SWI, both phase and magnitude data were acquired separately, with phase images filtered to enhance local changes of susceptibility effect. Phase masks were generated to highlight susceptibility properties and magnitude images were multiplied by phase masks, creating SWI.[2, 22, 23] For better venous contrast, minimum-intensity projection (mIP) images were made from 6 consecutive images.

For ASL perfusion imaging, quantitative CBF was calculated using M0 images.[21] CBF was calculated from whole brain data.

Regions of Interest

Regions of interest (ROIs) were placed at basal ganglia (BG), genu of the corpus callosum and gray matter (GM) and white matter (WM) of the frontal lobe (FL) and occipital lobe (OL) by one neuroradiologist (10 years of experience as a neuroradiologist) and differences in signal intensity on SWI were evaluated between NV and HV (Fig. 1). Contrast of the vein compared with adjacent cerebral parenchyma (CV) was evaluated in the perpendicular plane against the long axis of veins using 3-dimensional ROI. Three-dimensional ROIs were arbitrarily selected on bilateral superficial and deep cerebral veins and evaluated using ImageJ software

(http://rsb.info.nih.gov/ij/) (Fig. 2).

Statistical Analyses

Signal intensities of ROIs between NV and HV were compared. CV was also compared between NV and HV. Wilcoxon's signed rank test was applied for statistical analyses. Values of $P<0.05$ were considered statistically significant.

Results

Mild numbness in a limb was seen during hyperventilation in 2 of the 6 volunteers, but this rapidly improved with cessation of hyperventilation. No volunteers showed any other neurological abnormalities.

Mean values of whole brain CBF_{HV} decreased compared with those of CBF_{NV} and the decrease rate was 29.1 ±4.6% ($p=0.016$) (Table 1). The decrease rate for CBF was derived from the following equation: $[CBF_{NV} – CBF_{HV}]/CBF_{NV} \times 100$.

SWI showed marked decreases in signal intensity during HV (Fig. 3). Decrease rates for signal intensities in ROIs are shown in Table 2. Decrease rate was derived from the following equation: $[ROI_{NV} – ROI_{HV}]/ROI_{NV} \times 100$. $FL\text{-}GM_{HV}$ and $OL\text{-}GM_{HV}$ showed significant signal decreases compared with $FL\text{-}GM_{NV}$ and $OL\text{-}GM_{NV}$,

respectively (p=0.018, p=0.017). The rate of increase for venous contrast was obtained from the following equation. $[CV_{HV} - CV_{NV}]/CV_{NV} \times 100$. CV_{HV} was prominently increased compared with CV_{NV} (56.2 ±52.8%) (p=0.00019) (Table 3).

Discussion

SWI sensitively reflected CBF decreases under HV in this study. Decreases in BOLD signals reflect increased deoxyhemoglobin content and decreased local blood flow.[7] HV decreases CBF by vasoconstriction, but cerebral oxygen consumption under voluntary HV does not change in healthy persons.[24] Reduced CBF and unaltered oxygen metabolism is resolved by increasing oxygen extraction. Increased oxygen extraction is likely to be behind BOLD signal decreases during HV.[13, 15] Our results revealed significant decreases in signals for SWI under HV as compared with NV.

The most significant changes between NV and HV were seen in CV. The mask of phase images is used in postprocessing when creating SWI, which makes SWI sensitive to small BOLD changes. Magnitude images are multiplied by the mask of phase images, so BOLD effect of venous structures will be intensified without signal changes in magnitude images where veins are not present.[3] We thus suppose that CV has greatly changed as a result of CBF decreases compared with ROIs.

The contribution of these results to clinical practice has not been definitively established. In clinical studies, reduced intensities of transcerebral veins on T2*-weighted imaging were observed in regions with severe hemodynamic impairment.[25] The presence of hypointense abnormal transcerebral veins was significantly correlated with the occurrence of subsequent hemorrhagic transformation after ischemia.[25] Reduced CBF under HV differs from pathological CBF decreases such as seen in cerebral infarction, but asymmetrical hypointensities of venous structures on SWI might be associated with CBF decrease,[5, 26] and might thus provide useful information in clinical situations.

Several limitations in this study must be addressed. Numbness was seen in one-third of healthy volunteers. We could not perform whole-brain analysis of SWI, since this requires a longer scan time, which was deemed to have an unacceptable risk of causing subject distress. CBF reductions were calculated from whole-brain images, since ASL perfusion imaging covered the whole brain, whereas SWI covered only part of the brain.

Second, end-tidal CO_2, which reflects $PaCO_2$, was not directly monitored in this study. A state of hypocapnia was induced by voluntary hyperventilation. Although respiratory rate was monitored, the extent of $PaCO_2$ changes is likely to be more

informative, as such changes would have influenced CBF changes since the degree of hypocapnia induced by HV varies widely between individuals. Measurement of CBF on ASL perfusion imaging was performed in substitution for end-tidal CO_2 in this study, and a 29.1 ±4.6% CBF decrease was measured. However, if HV is continued for longer, subsequent recovery of CBF will be observed, influencing CBF data.[27] Consideration of cerebral blood volume and cerebral metabolic rate of oxygen is also indispensable for evaluation of SWI.[28] However, since HV does not alter cerebral oxygen consumption in healthy subjects,[15] ASL perfusion imaging might add more information for interpreting SWI.

In conclusion, SWI sensitively reflects hyperventilation-induced decreases in CBF and the results of our study might add to the interpretation of SWI in clinical practices, since CBF decreases might also influence on signal changes in SWI.

References

1. J. R. Reichenbach, R. Venkatesan, D. J. Schillinger, D. K. Kido and E. M. Haacke Small vessels in the human brain: MR venography with deoxyhemoglobin as an intrinsic contrast agent. *Radiology* 1997;204:272-277.

2. E. M. Haacke, Y. Xu, Y. C. Cheng and J. R. Reichenbach Susceptibility weighted imaging (SWI). *Magn Reson Med* 2004;52:612-618.

3. B. C. Lee, K. D. Vo, D. K. Kido, P. Mukherjee, J. Reichenbach, W. Lin, M. S. Yoon and M. Haacke MR high-resolution blood oxygenation level-dependent venography of occult (low-flow) vascular lesions. *AJNR Am J Neuroradiol* 1999;20:1239-1242.

4. M. Barth, I. M. Nobauer-Huhmann, J. R. Reichenbach, V. Mlynarik, A. Schoggl, C. Matula and S. Trattnig High-resolution three-dimensional contrast-enhanced blood oxygenation level-dependent magnetic resonance venography of brain tumors at 3 Tesla: first clinical experience and comparison with 1.5 Tesla. *Invest Radiol* 2003;38:409-414.

5. M. Hermier and N. Nighoghossian Contribution of susceptibility-weighted imaging to acute stroke assessment. *Stroke* 2004;35:1989-1994.

6. K. A. Tong, S. Ashwal, B. A. Holshouser, J. P. Nickerson, C. J. Wall, L. A.

Shutter, R. J. Osterdock, E. M. Haacke and D. Kido Diffuse axonal injury in children: clinical correlation with hemorrhagic lesions. *Ann Neurol* 2004;56:36-50.

7. S. Ogawa, T. M. Lee, A. R. Kay and D. W. Tank Brain magnetic resonance imaging with contrast dependent on blood oxygenation. *Proc Natl Acad Sci U S A* 1990;87:9868-9872.

8. L. J. Kemna and S. Posse Effect of Respiratory CO2 Changes on the Temporal Dynamics of the Hemodynamic Response in Functional MR Imaging. *NeuroImage* 2001;14:642-649.

9. S. P. Robinson, F. A. Howe and J. R. Griffiths Noninvasive monitoring of carbogen-induced changes in tumor blood flow and oxygenation by functional magnetic resonance imaging. *Int J Radiat Oncol Biol Phys* 1995;33:855-859.

10. A. Rauscher, J. Sedlacik, M. Barth, E. M. Haacke and J. R. Reichenbach Nonnvasive assessment of vascular architecture and function during modulated blood oxygenation using susceptibility weighted magnetic resonance imaging. *Magn Reson Med* 2005;54:87-95.

11. K. M. Sicard and T. Q. Duong Effects of hypoxia, hyperoxia, and hypercapnia on baseline and stimulus-evoked BOLD, CBF, and CMRO2 in spontaneously breathing animals. *NeuroImage* 2005;25:850-858.

12. M. Weckesser, S. Posse, U. Olthoff, L. Kemna, S. Dager and H. W. Muller-Gartner Functional imaging of the visual cortex with bold-contrast MRI: hyperventilation decreases signal response. *Magn Reson Med* 1999;41:213-216.

13. S. Naganawa, D. G. Norris, S. Zysset and T. Mildner Regional differences of fMR signal changes induced by hyperventilation: comparison between SE-EPI and GE-EPI at 3-T. *J Magn Reson Imaging* 2002;15:23-30.

14. R. G. Wise, K. Ide, M. J. Poulin and I. Tracey Resting fluctuations in arterial carbon dioxide induce significant low frequency variations in BOLD signal. *Neuroimage* 2004;21:1652-1664.

15. S. Posse, U. Olthoff, M. Weckesser, L. Jancke, H. W. Muller-Gartner and S. R. Dager Regional dynamic signal changes during controlled hyperventilation assessed with blood oxygen level-dependent functional MR imaging. *AJNR Am J Neuroradiol* 1997;18:1763-1770.

16. K. Ide, M. Eliasziw and M. J. Poulin The relationship between middle cerebral artery blood velocity and end-tidal PCO2 in the hypocapnic-hypercapnic range in humans. *J Appl Physiol* 2003;95:129-137.

17. J. R. Meno, T. S. Nguyen, E. M. Jensen, G. Alexander West, L. Groysman, D. K. Kung, A. C. Ngai, G. W. Britz and H. R. Winn Effect of caffeine on cerebral blood

flow response to somatosensory stimulation. *J Cereb Blood Flow Metab* 2005;25:775-784.

18. T. A. Mulderink, D. R. Gitelman, M. M. Mesulam and T. B. Parrish On the use of caffeine as a contrast booster for BOLD fMRI studies. *Neuroimage* 2002;15:37-44.

19. T. T. Liu, Y. Behzadi, K. Restom, K. Uludag, K. Lu, G. T. Buracas, D. J. Dubowitz and R. B. Buxton Caffeine alters the temporal dynamics of the visual BOLD response. *Neuroimage* 2004;23:1402-1413.

20. E. M. Haacke, C. Hu, T. Parrish and Y. Xu Whole brain stress test using caffeine: effects on fMRI and SWI at 3 T. *Proc. Int. Soc. Magn. Reson. Med* 2003;1731.

21. J. Wang, G. K. Aguirre, D. Y. Kimberg, A. C. Roc, L. Li and J. A. Detre Arterial spin labeling perfusion fMRI with very low task frequency. *Magn Reson Med* 2003;49:796-802.

22. J. R. Reichenbach, R. Venkatesan, D. A. Yablonskiy, M. R. Thompson, S. Lai and E. M. Haacke Theory and application of static field inhomogeneity effects in gradient-echo imaging. *J Magn Reson Imaging* 1997;7:266-279.

23. V. Sehgal, Z. Delproposto, E. M. Haacke, K. A. Tong, N. Wycliffe, D. K. Kido, Y. Xu, J. Neelavalli, D. Haddar and J. R. Reichenbach Clinical applications of neuroimaging with susceptibility-weighted imaging. *J Magn Reson Imaging*

2005;22:439-450.

24. P. C. van Rijen, P. R. Luyten, J. W. van der Sprenkel, V. Kraaier, A. C. van Huffelen, C. A. Tulleken and J. A. den Hollander 1H and 31P NMR measurement of cerebral lactate, high-energy phosphate levels, and pH in humans during voluntary hyperventilation: associated EEG, capnographic, and Doppler findings. *Magn Reson Med* 1989;10:182-193.

25. M. Hermier, N. Nighoghossian, L. Derex, P. Adeleine, M. Wiart, Y. Berthezene, F. Cotton, J. B. Pialat, P. Dardel, J. Honnorat, P. Trouillas and J. C. Froment Hypointense transcerebral veins at T2*-weighted MRI: a marker of hemorrhagic transformation risk in patients treated with intravenous tissue plasminogen activator. *J Cereb Blood Flow Metab* 2003;23:1362-1370.

26. H. An and W. Lin Cerebral oxygen extraction fraction and cerebral venous blood volume measurements using MRI: effects of magnetic field variation. *Magn Reson Med* 2002;47:958-966.

27. A. J. Johnston, L. A. Steiner, M. Balestreri, A. K. Gupta and D. K. Menon Hyperoxia and the cerebral hemodynamic responses to moderate hyperventilation. *Acta Anaesthesiol Scand* 2003;47:391-396.

28. J. R. Reichenbach and E. M. Haacke High-resolution BOLD venographic

imaging: a window into brain function. *NMR Biomed* 2001;14:453-467.

Table 1

CBF values calculated from ASL perfusion imaging and changes between NV and HV.

CBF_{NV}	CBF_{HV}	CBF Decrease $Rate_{HV-NV}$
52.8 ±8.0 ml/100 g/min	37.6 ±7.3 ml/100 g/min	29.1 ±4.6 %

p=0.016

Note: Values were derived from ASL perfusion imaging covering the whole brain.

Table 2

Signal intensity changes of ROIs between NV and HV.

ROI	BG	Genu	FL-GM	FL-WM	OL-GM	OL-WM
Decrease rate (%)	5.1 ±5.4	4.8 ±7.9	4.6 ±6.1*	3.4 ±5.7	5.3 ±5.7*	4.3 ±7.0

BG, basal ganglia; FL, frontal lobe; OL, occipital lobe; GM, gray matter; WM, white matter

*p<0.05

Table 3

Venous contrast of 3D-ROIs and changes between normal ventilation and hyperventilation.

CV_{NV}	CV_{HV}	Increase Rate of CV (%)
0.64 ±0.14	0.43 ±0.11	56.2 ±52.8

p=0.00019

Figure Legends

Figure 1

Minimum intensity projection of SWI [TR 27 ms; TE 20 ms]. Regions of interest (ROIs) were placed at basal ganglia (BG), genu, and gray matter (GM) and white matter (WM) of frontal lobes (FL) and occipital lobes (OL) (a, b). The same ROIs were applied for SWI under normal ventilation and hyperventilation.

1: BG; 2: genu; 3, 4: FL-GM, 5, 6: FL-WM; 7, 8: OL-WM; 9, 10: OL-GM.

Figure 2

Venous contrast compared with adjacent brain parenchyma (CV) was evaluated in the perpendicular plane against the long axis of veins using 3D-ROI. 3D-ROIs were arbitrarily selected on bilateral superficial and deep cerebral veins. Part of a minimum-intensity projection of SWI [TR 27 ms; TE 20 ms] under normal ventilation (a) and hyperventilation (b) is shown. Superficial cerebral vein was more clearly depicted under hyperventilation compared with under normal ventilation (arrows). Better contrast to surrounding cerebral parenchyma was seen on 3D-ROI of a superficial vein (arrowheads) under hyperventilation (d) than under normal ventilation (c).

Figure 3

Minimum-intensity projection of SWI [TR 27 ms; TE 20 ms] under normal ventilation (a) and hyperventilation (b). Venous structures were prominently conspicuous under hyperventilation.

Figure 1

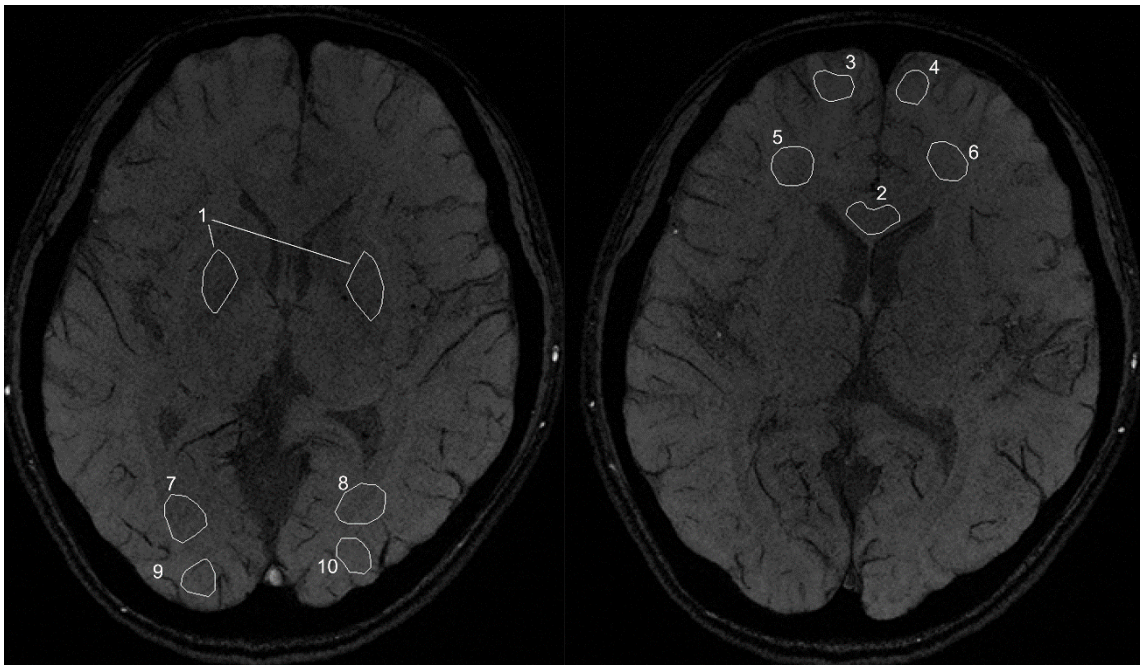

Figure 2

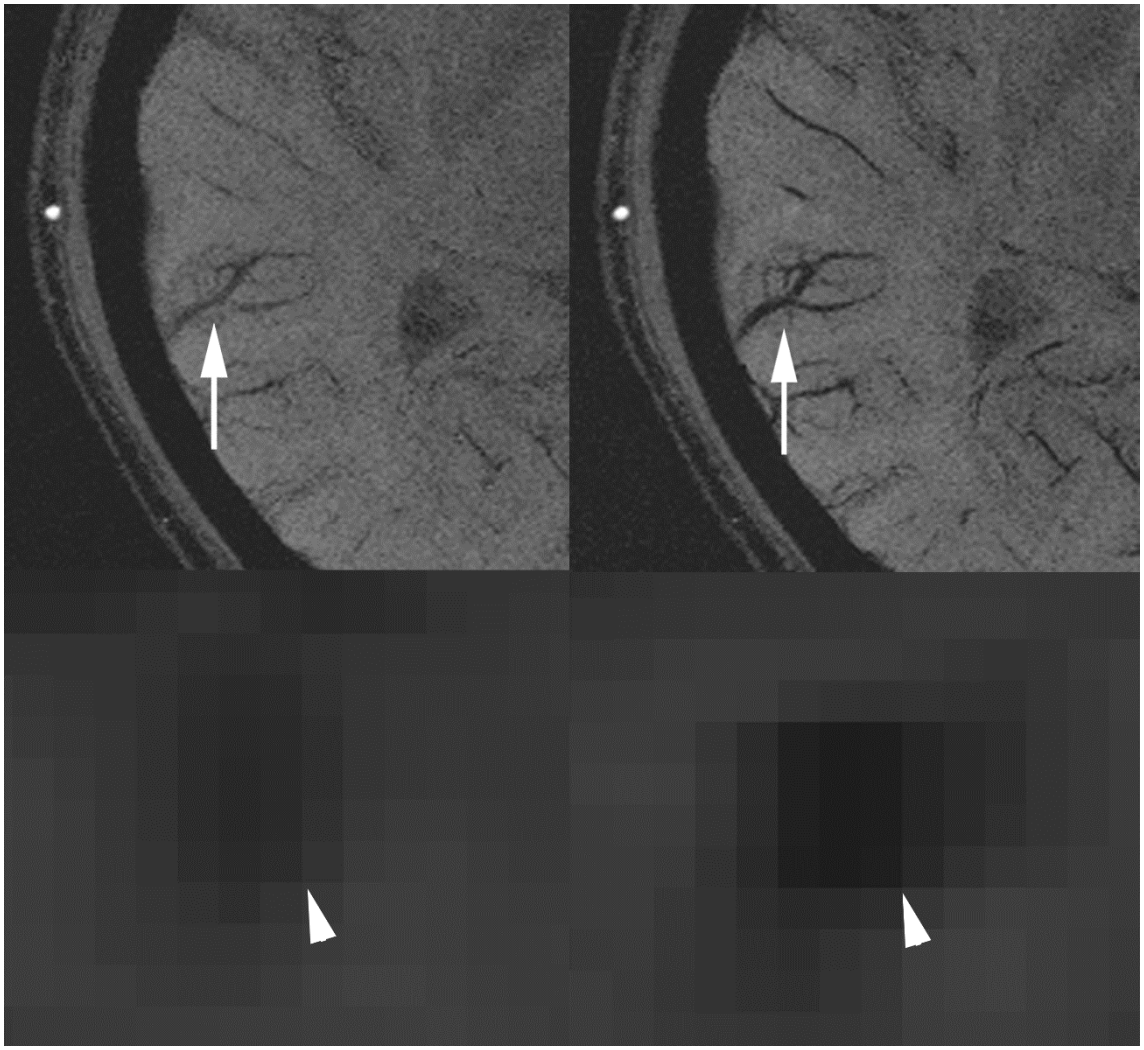

Figure 3